ESMO GOOD SCIENCE BETTER MEDICINE BEST PRACTICE

IOTECH IMMUNO-ONCOLOGY AND TECHNOLOGY

ORIGINAL ARTICLE

Effective generation of tumor-infiltrating lymphocyte products from metastatic non-small-cell lung cancer (NSCLC) lesions irrespective of location and previous treatments

S. M. Castenmiller[1,2†], R. de Groot[1,2†], A. Guislain[1,2], K. Monkhorst[3], K. J. Hartemink[4], A. A. F. A. Veenhof[4], E. F. Smit[5], J. B. A. G. Haanen[6] & M. C. Wolkers[1,2*]

[1]Sanquin Blood Supply, Department of Hematopoiesis and Landsteiner Laboratory, Amsterdam UMC, Amsterdam; [2]Oncode Institute, Utrecht; Departments of [3]Pathology; [4]Surgery; [5]Thoracic Oncology; [6]Medical Oncology, Netherlands Cancer Institute-Antoni van Leeuwenhoek Hospital (NKI-AvL), Amsterdam, The Netherlands

Available online 22 June 2022

Background: Non-small-cell lung cancer (NSCLC) is the leading cause of cancer-related mortality worldwide. Because current treatment regimens show limited success rates, alternative therapeutic approaches are needed. We recently showed that treatment-naïve, stage I/II primary NSCLC tumors contain a high percentage of tumor-reactive T cells, and that these tumor-reactive T cells can be effectively expanded and used for the generation of autologous tumor-infiltrating T cell (TIL) therapy. Whether these promising findings also hold true for metastatic lesions is unknown yet critical for translation into the clinic.

Materials and methods: We studied the lymphocyte composition using flow cytometry from 27 metastatic NSCLC lesions obtained from different locations and from patients with different histories of treatment regimens. We determined the expansion capacity of TILs with the clinically approved protocol, and measured their capacity to produce the key pro-inflammatory cytokines interferon-γ, tumor necrosis factor and interleukin 2 and to express CD137 upon co-culture of expanded TILs with the autologous tumor digest.

Results: The overall number and composition of lymphocyte infiltrates from the various metastatic lesions was by and large comparable to that of early-stage primary NSCLC tumors. We effectively expanded TILs from all metastatic NSCLC lesions to numbers that were compatible with TIL transfusion, irrespective of the location of the metastasis and of the previous treatment. Importantly, 16 of 21 (76%) tested TIL products displayed antitumoral activity, and several contained polyfunctional T cells.

Conclusions: Metastatic NSCLC lesions constitute a viable source for the generation of tumor-reactive TIL products for therapeutic purposes irrespective of their location and the pre-treatment regimens.

Key words: non-small-cell lung cancer, T cells, tumor-infiltrating lymphocytes, metastatic lesions, TIL therapy

INTRODUCTION

Lung cancer is the most common cause of cancer-related mortality worldwide.[1] Non-small-cell lung cancer (NSCLC) accounts for 85% of patients diagnosed with lung cancer.[2] New treatment strategies such as targeted therapy,[3,4] immunotherapy[5-7] or combined chemo- and immunotherapy have been developed.[8-11] Nevertheless, the 5-year survival rate for NSCLC patients is still dismal.[12] Therefore, alternative treatment options for late-stage NSCLC patients are required.

The high somatic mutational rate of NSCLC tumors makes them immunogenic,[13] and a high percentage of tumor-infiltrating T cells (TILs) in treatment-naïve patients,[14-16] with tumor specificity and cytotoxic activity,[17,18] was shown by us and others. Adoptive TIL therapy for NSCLC patients could thus represent a viable alternative to current therapies. TIL therapy relies on a 4-6 week *in vitro* expansion of autologous TILs that are then re-infused into pre-conditioned patients.[19] In stage III/IV melanoma patients, adoptive TIL therapy achieved an astounding overall response rate of >50% and a complete response rate of 20%.[20-23] The similarly high immunogenicity of NSCLC implies that also NSCLC patients could benefit from TIL therapy.

We previously reported that tumor-reactive TIL products can be efficiently generated from treatment-naïve, early-stage primary NSCLC tumor lesions.[14] Importantly, >70%

*Correspondence to: Dr Monika C. Wolkers, Sanquin Research, Department of Hematopoiesis, Plesmanlaan 125, 1066 CX Amsterdam, The Netherlands. Tel: +31-6-24268490; Fax: +31-20-5123474

E-mail: m.wolkers@sanquin.nl (M. C. Wolkers).

†These authors contributed equally.

of expanded TILs displayed tumor reactivity when exposed to autologous tumor digest, i.e. they produced at least one of the key pro-inflammatory cytokines interferon-γ (IFN-γ), tumor necrosis factor (TNF) and interleukin 2 (IL-2), and expressed the costimulatory receptor CD137, indicative of T cell receptor (TCR) triggering.[14,24] Intriguingly, 25% of expanded TILs were polyfunctional and produced more than one cytokine,[14] which correlates with highly functional effector T cells.[25,26] Our study thus demonstrates that tumor-reactive TIL products can be readily generated from treatment-naïve primary NSCLC tumors.

Importantly, a recent phase I clinical trial for TIL therapy in late-stage anti-programmed death-1 (PD-1)-refractory NSCLC patients showed striking therapeutic effects.[27] In 11 out of 16 patients (68.8%), tumors regressed within 1 month after treatment.[27] Two patients (12.5%) had a complete response that was ongoing for at least 1.5 years.[27] These exciting results thus highlight the potential of TIL therapy for NSCLC patients. However, to effectively implement TIL therapy for NSCLC patients, it is paramount to define which patient groups are likely to benefit from this treatment. Historic cohorts demonstrated the feasibility of TIL expansion, but this was based on long expansion protocols, and included lung metastases only.[28] Furthermore, patients receive different treatments (pre-treatment regimen), such as (immuno)chemotherapy, immune checkpoint inhibitors or small molecule inhibitors. An update that defines the compatibility of TIL expansion with currently administered treatment regimens is thus needed. Also the location of metastatic tumor lesions[29] may influence TIL expansion and tumor reactivity. Collecting such data is thus critical to implement TIL therapy for NSCLC patients in the clinic.

Here, we provide an in-depth analysis of the lymphocyte composition of metastatic lesions from 27 late-stage NSCLC patients originating from different metastatic locations, and who received various (or no) pre-treatment regimens. We show that TILs effectively expand from all metastatic tumor lesions. Importantly, most TIL products contained tumor-reactive T cells, as defined by cytokine production in response to autologous tumor digests. Our study thus demonstrates that tumor-reactive TIL products can be generated for therapeutic purposes from late-stage NSCLC lesions, irrespective of the pre-treatment regimen and the location of the metastatic tumor lesion.

MATERIALS AND METHODS

Patient cohort and study design

Between October 2017 and April 2020, 27 late-stage NSCLC patients were included. The study protocol was designed to determine the TIL phenotype ($n = 25$), the capacity to expand TILs ($n = 27$) and the presence of tumor-reactive T cells in TIL products ($n = 22$). Patients' characteristics, origin of metastasis, pre-treatment regimens and time between the last treatment and surgery are depicted in Table 1. When tumor lesions were too small ($n = 5$), *ex vivo* TIL phenotype ($n = 2$) and the tumor reactivity to tumor digest ($n = 5$) could not be tested. The study was carried out according to the Declaration of Helsinki (seventh revision, 2013), with consent of the Institutional Review Board of the Netherlands Cancer Institute-Antoni van Leeuwenhoek Hospital (NKI-AvL), Amsterdam, The Netherlands. Tumor tissue was obtained directly after surgery, transported at 20°C in RPMI-1640 medium (Gibco, ThermoFisher Scientific, Landsmeer, the Netherlands) containing 50 μg/ml gentamycin (Sigma-Aldrich, Merck, Schiphol-Rijk, the Netherlands), 12.5 μg/ml fungizone (Amphotericin B, Gibco, Landsmeer, the Netherlands) and 20% fetal bovine serum (FBS, Bodego, Bodinco BV, Alkmaar, the Netherlands), weighed and processed within 4 hours. Tumor stage and differentiation, weight of obtained tissue and total tumor size are reported in Table 2. Surgery was not always carried out for diagnostic purposes; therefore, tumor characteristics were not determined for each patient.

Tissue digestion

Tissue digestion and red blood cell lysis were carried out as we previously reported.[14] Live and dead cells were manually counted (hemocytometer) with trypan blue solution (Sigma, Schiphol-Rijk, the Netherlands). A total of 1-2 $\times$ 10^6 live cells were used for flow cytometry analysis, and 1-3 $\times$ 10^6 live cells were cultured. The remaining digest was cryopreserved until further use.

T cell expansion

Two to three wells containing 0.5-1 $\times$ 10^6 live cells from the tissue digest were cultured for 10-13 days in 24-well plates in 20/80 T-cell mixed media (Miltenyi, Leiden, the Netherlands) containing 5% human serum (Sanquin, Amsterdam, the Netherlands), 5% FBS, 50 μg/ml gentamycin, 1.25 μg/ml fungizone and 6000 IU human recombinant (hr) IL-2 (Proleukin, Novartis, Amsterdam, the Netherlands) [pre-rapid expansion phase (pre-REP)] at 37°C and 5% CO_2. Medium was refreshed on day 7, 9 and 11 in pre-REP. When a monolayer of cells was observed in the entire well, cells were split into two wells. When >30% cells stopped dividing (determined as cell rounding), cells were harvested, counted and prepared for an additional REP culture period of 10-13 days. A total of 2 $\times$ 10^5 live cells/well (1-3 wells/patient) were co-cultured with 5-10 $\times$ 10^6 irradiated peripheral blood mononuclear cells (PBMCs) pooled from 15 healthy blood donors in a 24-well plate, 30 ng/ml anti-CD3 antibody (OKT-3) (Miltenyi Biotec, Leiden, the Netherlands) and 3000 IU/ml hrIL-2. Typically, cells were passaged when a monolayer of cells was observed in the wells during the REP (generally every other day) and harvested, washed and counted on day 10-13 after REP, based on visual assessment of T cell proliferation state as described previously. Cells were used immediately, or cryo-preserved in RPMI-1640 medium containing 10% dimethyl sulfoxide (Corning, Amsterdam, the Netherlands) and 40% FBS until further use.

T cell activation

Fresh or defrosted REP TILs were counted and pre-stained in fluorescence-activated cell sorter (FACS) buffer with anti-CD4 BUV496 and anti-CD8 BUV805 (BD, Vianen, the

Table 1. Patient characteristics

Patient	Gender (M/F)	Age at surgery (years)	Smoking history (cigarettes per day)	Clinical stage (TNM7[a])	Tumor lesion site	Pre-treatment regimen	Last treatment (days/ months before surgery)
1	M	64	Unknown	IVA	Lung	Nivolumab + ipilimumab (immunotherapy)	6 months
2	F	64	No (never)	IVA	Lung	Cis/pem + carbo/pem (chemotherapy)	12 days
3	M	45	Yes (unknown)	IIIA	Lung/lymph node	Treatment naïve	
4	M	55	Yes (16/day)	IV	Lymph node	Treatment naïve	
5	F	48	Yes (20/day)	IV	Lung	Cis/pem (chemotherapy)	Unknown
6	F	50	Yes (20/day)	IV	Lymph node	Nivolumab (immunotherapy)	4 months
7	M	58	Yes (6/day)	IV	Lung	Pembrolizumab (immunotherapy)	1 month
8	F	57	No (never)	IV	Lung	Pembrolizumab (immunotherapy)	1 month
9	M	55	No (never)	IV	Lung	Erlotinib/osimertinib (EGFR inhibitor)	Continued
10	F	39	Yes (25/day)	IV	Adrenal gland	Pembrolizumab (immunotherapy)	12 days
11	F	60	Yes (13/day)	IV	Subcutaneous tissue—hip	Treatment naïve	
12	F	69	No (never)	IV	Liver	EGFR inhibitor	14 days
13	M	53	No (never)	IV	Adrenal gland	Alectinib (ALK inhibitor)	15 months
14	F	70	Yes (20/day)	IV	Adrenal gland	Carbo/pem (chemotherapy)	17 months
15	M	66	Yes (unknown)	IV	Subcutaneous tissue—skin	Cis/gem + nivolumab (chemo-immuno)	1 month (immuno)
16	M	87	Yes (8/day)	IV	Adrenal gland	Crizotinib (ALK inhibitor)	14 days
17	F	73	No (never)	IV	Adrenal gland	Osimertinib (EGFR inhibitor)	Continued
18	M	60	Yes (30/day)	IV	Spleen	CRT (chemo) + nivolumab (immunotherapy)	20 days (immuno)
19	F	47	Yes (5/day)	IV	Adrenal gland	Nivolumab + anti-LAG3 (immunotherapy)	19 days
20	M	55	Yes (4/day)	IV	Lung	Carbo/pem + pembrolizumab (chemo-immuno)	1 month (immuno)
21	F	40	Yes (25/day)	IV	Adrenal gland	Cis/gem + pembrolizumab (chemo-immuno)	4 days (immuno)
22	M	58	Yes (4/day)	IV	Lung	Cis/eto/carbo + nivolumab (chemo-immuno)	14 days (immuno)
23	F	66	Yes (19/day)	IV	Lung	Pembrolizumab (immunotherapy)	1 month
24	M	77	Yes (10/day)	IV	Lung	Treatment naïve	
25	M	73	Yes (10/day)	IV	Adrenal gland	Carbo/pem (chemotherapy)	14 months
26	F	65	Yes (25/day)	IV	Lung	Pembrolizumab (immunotherapy)	1 month
27	F	72	Yes (5/day)	IV	Lung	Cis/pem (chemotherapy)	Unknown

ALK, anaplastic lymphoma kinase; carbo, carboplatin; cis, cisplatin; CRT, chemoradiotherapy; EGFR, epidermal growth factor receptor; eto, etoposide; F, female; LAG3, lymphocyte activation gene-3; M, male; pem, pembrolizumab; TNM, tumor, nodes and metastasis.
[a]American Joint committee on Cancer: Lung Cancer Staging, seventh edition, 2009.

Netherlands) for 30 min at 4°C. Cells were washed once with FACS buffer, and once with 20/80 T-cell mixed media. A total of 1×10^5 live expanded TILs were co-cultured with 2×10^5 live tumor digest cells for 6 h at 37°C. Alternatively, expanded TILs were stimulated with 10 ng/ml phorbol myristate acetate (PMA) and 1 μg/ml ionomycin (Sigma-Aldrich), or cultured with T cell mixed media alone. After 1 h of co-culture, 1x Brefeldin A and 1x Monensin (Invitrogen, Landsmeer, the Netherlands) were added.

Flow cytometry

For *ex vivo* analysis, tumor digests were washed twice with FACS buffer and stained in FACS buffer for 30 min at 4°C with anti-CD3 PerCp-Cy5.5, anti-CD279 FITC, anti-CD103 FITC, anti-CD56 BV605, anti-CD27 BV510, anti-CD127 BV421, anti-CD279 BV421, anti-CD39 PE-Cy7, anti-CD103 PE-Cy7 and anti-CD25 PE (Biolegend, Amsterdam, the Netherlands), and with anti-CD8 BUV805, anti-CD45RA BUV737, anti-CD4 BUV496 and anti-CD69 BUV395 (BD). Live/dead fixable near-IR APC-Cy7 (Invitrogen) was included for dead cell exclusion. Cells were washed twice with FACS buffer and fixed for 30 min with Perm/Fix Foxp3 staining kit (Invitrogen) according to manufacturer's protocol. Cells were stained with anti-Foxp3 Alexa647, anti-CD137 Alexa647 or anti-CD137 PE-Cy7 (Biolegend) for 30 min at 4°C. Cells were resuspended in FACS buffer and passed through a 70-μm single-cell filter before flow cytometry analysis (Symphony A5, BD Biosciences, San Jose, CA). Expanded TILs were washed twice with FACS buffer and pre-stained with anti-CD4 BUV496 and anti-CD8 BUV805 as described previously. Anti-CD107 Alexa700 (BD) was added to the co-culture. After T cell activation, cells were washed twice with FACS buffer and stained with anti-CD3 PerCp-Cy5.5 and anti-CD279 BV421 (Biolegend) and live/dead fixable near-IR APC-Cy7 in FACS buffer for 30 min at 4°C. After two washes with FACS buffer, cells were fixed with Perm/Fix Foxp3 staining kit (Invitrogen) and then stained with anti-CD137 Alexa647 (Invitrogen), anti-CD154 BV510, anti-IFN-γ PE, anti-TNF-α BV785 and anti-IL-2 FITC (Biolegend) in PermWash buffer according to manufacturer's protocol. Cells were washed with FACS buffer and passed through a 70-μM single-cell filter before acquisition with the Symphony A5 flow cytometer (BD Biosciences). Flow cytometry settings were defined for each patient with single antibody stainings. Furthermore, a standardized PBMC sample pooled from four healthy donors that was cryo-preserved before the start of the study was included for each measurement. Data analysis was carried out with FlowJo Star 10.7.1 (BD, Ashland, OR).

Table 2. Tumor characteristics

Donor	Tumor differentiation	Pathology stage (TNM7[a])	PD-L1 status (determined at PA)	Biopsy weight (mg)	Tumor size (cm^3)
1	AC	ypT2bN0PL0/cT4N3M1a	ND	2140	4.7
2	AC	ypT2aN2PL0/dT4N2M1a	80%	670	3.2
3	AC	pT1bN2PL0	100%	1500	1.5
4	AC	ND	70%	1408	2.0
5	NOS	cT3N1M1c/ypT0N0	ND	320	1.5
6	AC	cT3N3M1b	1%	1000	3.5
7	AC	ND	90%	230	2.4
8	AC	ypT1aN0PL0	5%	800	1.0
9	AC	ypT1cN0M1aPL0	<1%	500	2.5
10	AC	cT3N2M1	<1%	600	2.6
11	AC	ND	<1%	1200	1.2
12	AC	ND	<1%	4000	4.6
13	AC	ND	100%	250	3.0
14	NOS	cT1cN2M1c	70%	1810	7.5
15	SSC	cTxN3M1b	<1%	8810	4.5
16	AC	ND	30%	Unknown	7.5
17	AC	pT2N2PL1M0	1%	Unknown	2.8
18	AC	ND	80%	8590	7.1
19	AC	ND	2%	580	3.5
20	AC	ypT0N1	70%	590	Unknown
21	AC	cT3N2M1	<1%	Unknown	1.7
22	SSC	pT2bN0PL1	50%	Unknown	4.2
23	AC	pT1bPL0	90%	150	1.9
24	AC	pT4N2PL1	ND	600	3.2
25	AC	cT1cN0M2	<1%	750	3.7
26	AC	ND	<1%	120	1.4
27	AC	ypT3PL1	<1%	420	1.2

AC, adenocarcinoma; NOS, NSCLC not otherwise specified; ND, not determined; PA, pathology; PD-L1, programmed death-ligand 1; SCC, squamous carcinoma; TNM, tumor, nodes and metastasis.
[a]American Joint committee on Cancer: Lung Cancer Staging, seventh edition, 2009.

Statistical analysis

Statistical analysis was carried out with GraphPad Prism 8.0.2 (Dotmatics, San Diego, CA). Data are shown as paired data points for each patient, or as single data points with box and whiskers showing maximum, 75th percentile, median, 25th percentile and minimum, unless otherwise stated. Overall significance was calculated with unpaired parametric *t*-test with a two-tailed *P* value, with ordinary two-way analysis of variance test or with paired parametric *t*-test with a two-tailed *P* value, and variance was calculated as standard deviation. The *P* value cut-offs were set on * = $P < 0.05$, ** = $P < 0.01$, *** = $P < 0.001$, **** = $P < 0.0001$.

RESULTS

Metastatic NSCLC tumor lesions contain a high number of T cell infiltrates

Twenty-seven late-stage NSCLC patients (13 male, 14 female) were included in this study. Patients were between 39 and 87 years of age (average 60.2 years), with clinical stage III ($n = 1$) and stage IV ($n = 26$) according to TNM (tumor, nodes and metastasis) seventh edition staging system for NSCLC. Twenty patients (74%) had a history of smoking. Tumor size ranged from T1a to T4, and was specified as adenocarcinoma ($n = 23$), squamous carcinoma ($n = 2$) and NSCLC not otherwise specified ($n = 2$) (Table 1). On average, 1610 mg tumor tissue was obtained, ranging from 120 to 8810 mg. Single-cell suspensions were generated with the clinically approved digestion protocol, and the number of viable cells and of T cell infiltrates was determined. On average, we collected 41.2×10^6 (range 1.5-206×10^6) viable cells per gram tissue, which is comparable to numbers we obtained from early-stage primary tumor lesions (note that tumor lesions were identically processed)[14] (Figure 1A). Lymphocytes reached on average 17.0×10^6 cells per gram tissue (range 0.6-82.1×10^6 cells) (Supplementary Figures S1 and S2, available at https://doi.org/10.1016/j.iotech.2022.100090), of which most (71.4% ± 21.4%) were $CD3^+$ T cells, with on average 15.5×10^6 cells (range 0.2-70×10^6) per gram tissue (Figure 1A). Thus, the absolute number and percentage of $CD3^+$ T cell infiltrates resembled those of early-stage tumor lesions[14] (Figure 1A), albeit with a broader range. We therefore assessed whether pre-treatment regimens or the metastatic location influenced the T cell content. The cohort contained metastatic lesions from treatment-naïve ($n = 4$) patients and from patients pre-treated with immunotherapy ($n = 8$), chemotherapy ($n = 5$), a combination thereof ($n = 5$) or small molecule inhibitors anaplastic lymphoma kinase inhibitors ($n = 2$) and epidermal growth factor receptor inhibitors ($n = 3$) (Table 1). Metastatic tumor lesions originated from the lung ($n = 12$), lymph nodes ($n = 3$), adrenal gland ($n = 8$), liver ($n = 1$), spleen ($n = 1$) and subcutaneous tissue ($n = 2$) (Table 1). Neither metastatic location nor pre-treatment regimen showed clear

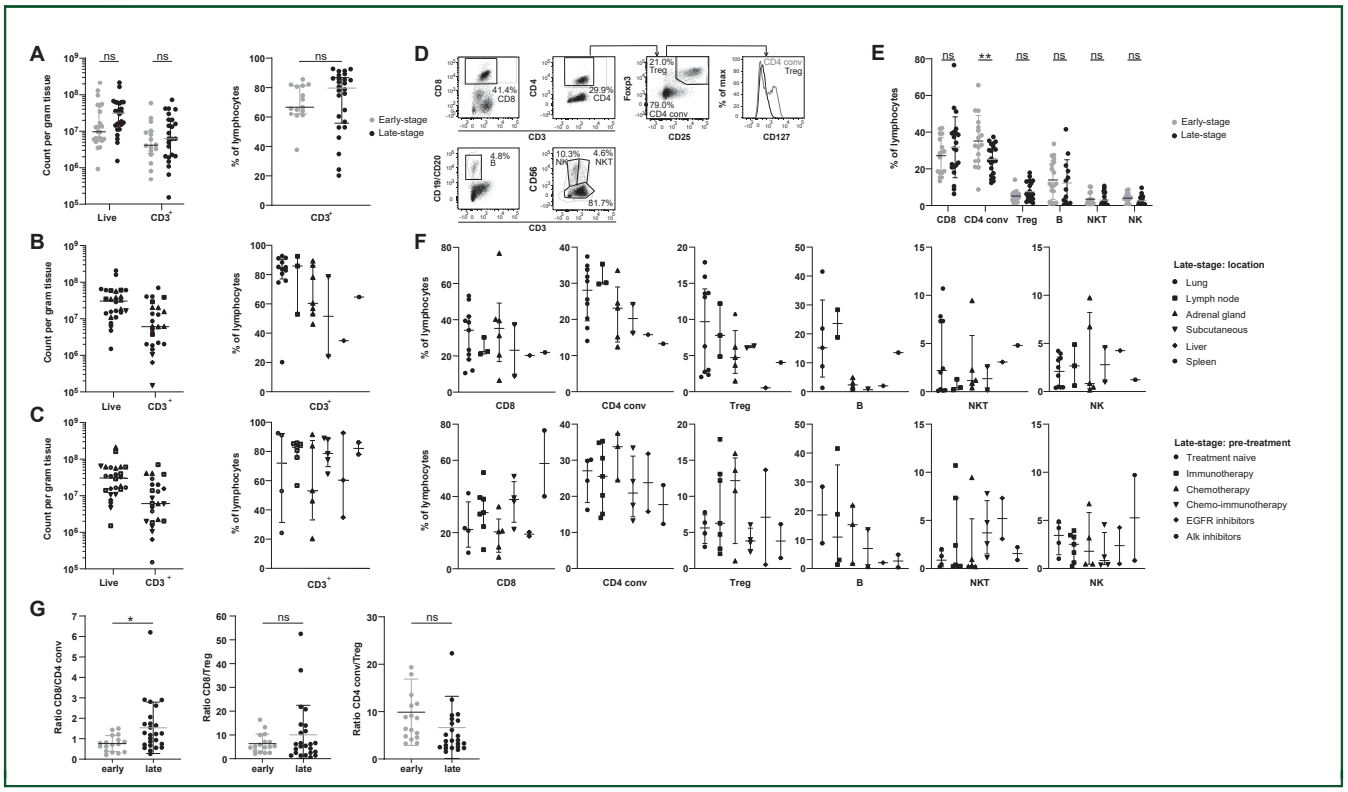

Figure 1. Effective isolation of lymphocytes from late-stage non-small-cell lung cancer (NSCLC) lesions, with similar lymphocyte distribution compared to early-stage NSCLC lesions. Single-cell suspensions were obtained by enzymatic digestion of metastatic lesions from late-stage NSCLC patients. Life cell count was assessed with trypan blue staining, and lymphocyte and $CD3^+$ percentage was determined by flow cytometry. (A-C) Left: Count of live and of $CD3^+$ T cells per gram tissue. Right: Percentage of $CD3^+$ T cells within the lymphocyte population. (A) Composition of the yield of live and $CD3^+$ T cells in tumor lesions from the late-stage NSCLC patients ($n = 27$, black) compared to treatment-naïve primary tumor lesions as reported previously ($n = 17$, gray).[14] (B) Comparison of the yield of live and of $CD3^+$ T cells from different tumor lesion sites, indicated as lung ($n = 12$), lymph node ($n = 3$), adrenal gland ($n = 8$), subcutaneous tissue ($n = 2$), liver ($n = 1$) and spleen ($n = 1$). (C) Comparison of different pre-treatment regimens, indicated as treatment naïve ($n = 4$), immunotherapy ($n = 8$), chemotherapy ($n = 5$), chemo-immunotherapy ($n = 5$), epidermal growth factor receptor (EGFR) inhibitors and anaplastic lymphoma kinase (ALK) inhibitors ($n = 2$). (D) Gating strategy for defining different lymphocyte populations (patient 13) as reported in E-G, indicated as $CD8^+$ T cells, $CD4^+$ T cells, regulatory T cells (Tregs), conventional $CD4^+$ T cells, B cells, natural killer (NK) cells and natural killer T (NKT) cells. (E) Lymphocyte composition from late-stage metastatic lesions (black, $n = 25$) compared to early-stage primary tumor lesions (gray, $n = 17$).[14] (F) Percentage of indicated lymphocyte populations between patients with different tumor lesion site (top) and different pre-treatment regimens (bottom). (G) Ratio of $CD8^+$ T cells over conventional $CD4^+$ T cells (left) and regulatory $CD4^+$ T cells (middle), and of conventional $CD4^+$ T cells over Tregs (right) in late-stage NSCLC lesions (black, $n = 25$) and early-stage primary NSCLC tumors (gray, $n = 17$).[14] Each dot represents one patient. All graphs show median with 25th and 75th percentile interval, except for B and C left panel where only median is shown. Significance was calculated with unpaired Student's *t*-test. $*P < 0.05$, $**P < 0.01$. Not significant (ns): $P \geq 0.05$.

differences in the overall yield of viable or $CD3^+$ T cells (Figure 1B and C). Thus, $CD3^+$ T cells can be readily obtained from late-stage NSCLC tumor lesions independently of treatment regimens and the metastatic location.

Conserved lymphocyte infiltration profile in late-stage metastatic NSCLC lesions

We next measured the lymphocyte composition in metastatic NSCLC tumors (gating strategy: Figure 1D).[14] Overall, the percentage of T cells, B cells, natural killer (NK) cells and natural killer T (NKT) cells in late-stage metastatic tumors resembled that of primary early-stage tumors (Figure 1E). $CD3^+$ T cells were most prevalent, with 31.8% ± 16.6% $CD8^+$ T cells, 25.1% ± 8.1% conventional $CD4^+$ T cells and 7.6% ± 5.0% regulatory T cells (Tregs) (Figure 1E). We observed a broader distribution in $CD8^+$ T cell and Treg percentages in metastatic lesions compared to primary tumors, yet without significant differences (Figure 1E). Conversely, the percentage of conventional $CD4^+$ T cell infiltrates was significantly lower in metastatic NSCLC lesions compared to early-stage tumors (Figure 1E; $P = 0.008$). Overall, albeit displaying trends, pre-treatment regimens and metastatic locations failed to show overt differences in lymphocyte infiltration (Figure 1F). Similarly, the ratio between $CD8^+$ T cells and Tregs, and between conventional $CD4^+$ T cells and Tregs was similar between metastatic and early-stage primary tumors (Figure 1G). However, the ratio between $CD8^+$ and conventional $CD4^+$ T cells shifted in late-stage tumors, with an average ratio of 1.54 (late-stage) to 0.8 (early-stage) (Figure 1G; $P = 0.02$). In conclusion, lymphocyte infiltrates are comparable between early-stage and late-stage tumors, except for a reduced ratio of conventional $CD4^+$ infiltrates in late-stage NSCLC tumors.

Metastatic lesions contain T cells with a memory and tissue residency profile

The T cell memory profile is an important indicator for T cell function. We therefore investigated the T cell profile in

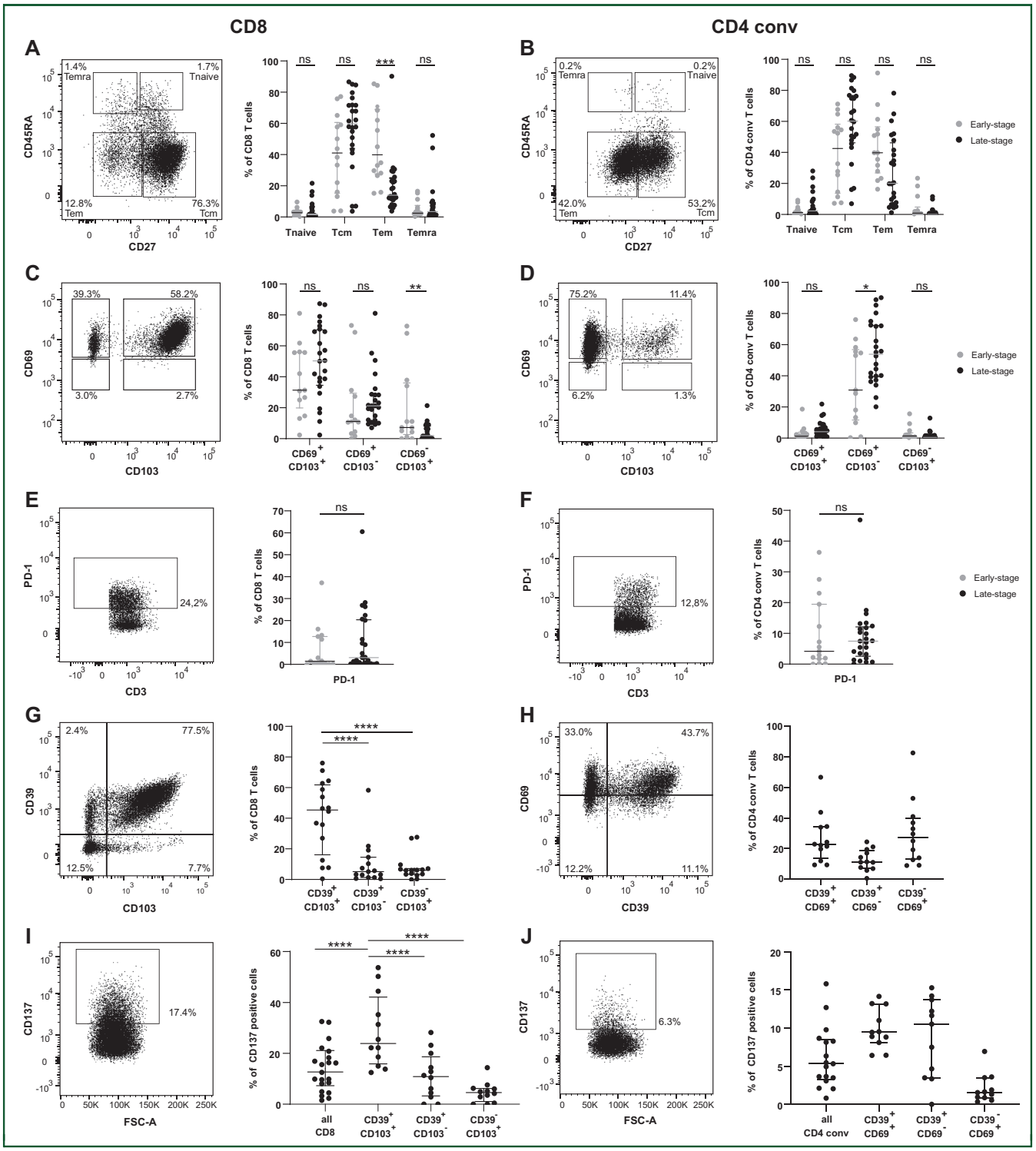

Figure 2. ***Ex vivo*** **memory status, tissue residency, activation and exhaustion marker expression in metastatic tumor lesions compared to primary early-stage tumor lesions.** (A, B) T cell memory status of tumor-infiltrating T cells (TILs) from late-stage (black, $n = 24$) and early-stage (gray, $n = 14$)[14] tumor lesions, as defined by their expression of CD27 and CD45RA. Left: Representative dot plot (patient 13). Right: The percentage of naïve T (Tnaive) ($CD27^+CD45RA^+$), central memory T (Tcm) ($CD27^+CD45RA^-$), effector memory T (Tem) ($CD27^-CD45RA^-$) and terminally differentiated effector memory T (Temra) ($CD27^-CD45RA^+$) for (A) $CD8^+$ T cells and (B) conventional $CD4^+$ T cells. (C, D) Comparison of expression of tissue-residency markers CD69 and CD103 on TILs from late-stage (black, $n = 24$) and early-stage (gray, $n = 13$).[14] Left: Representative dot plot (patient 13). Right: The percentage of $CD69^+CD103^+$, $CD69^+CD103^-$ and $CD69^-CD103^+$ for (C) $CD8^+$ T cells and (D) conventional $CD4^+$ T cells. (E, F) Programmed cell death protein 1 (PD-1) expression between late-stage (black, $n = 25$) and early-stage (gray, $n = 15$)[14] TILs. Left: Gating strategy for defining PD-1 expression (patient 13). Right: Percentage of PD-1 for (E) $CD8^+$ T cells and (F) conventional $CD4^+$ T cells. (G, H) CD39 expression in tissue-resident T cells. Left: Gating strategy for defining CD39 expression (patient 13). Right: Percentage of (G) CD39 and CD103 expression for $CD8^+$ T cells and (H) CD39 and CD69 expression for conventional $CD4^+$ T cells. (I, J) CD137 (4-IBB) expression, calculated as percentage of the subpopulation labeled on the *x*-axis. Left: Gating strategy for defining CD137 expression (patient 13). Right: CD137 expression in (I) CD39 and CD103-expressing cells for $CD8^+$ T cells and in (J) CD39 and CD69-expressing cells for conventional $CD4^+$ T cells. Each dot represents one patient. All graphs show median and 25th and 75th percentile interval. Significance was calculated with two-way analysis of variance test (Tukey's multiple comparison) (A-F) or unpaired Student's *t*-test (G-J). $^*P < 0.05$, $^{**}P < 0.01$, $^{***}P < 0.001$, $^{****}P < 0.0001$. Not significant (ns): $P \geq 0.05$.
FSC-A, forward scatter area.

metastatic lesions by measuring the expression of CD27 and CD45RA to distinguish $CD27^+CD45RA^+$ naïve (Tnaive), $CD27^+CD45RA^-$ central memory (Tcm), $CD27^-CD45RA^-$ effector memory (Tem) and $CD27^-CD45RA^+$ terminally differentiated effector memory (Temra) cells (Figure 2A and B). The percentages of $CD8^+$ Tem cells were substantially reduced in late-stage TILs when compared to early-stage NSCLC TILs ($P = 0.0003$), concomitant with a slight but non-significant increase in $CD8^+$ Tcm cells (Figure 2A). A similar yet non-significant shift toward Tcm away from Tem was found for $CD4^+$ T cells (Figure 2B; $P = 0.09$). The percentages of Tnaive and Temra cells in the $CD8^+$ and $CD4^+$ T cell compartment remained stable (Figure 2A and B).

Tissue residency markers can be used as clinical parameters for patients with lung tumor lesions.[30] We found high percentages of $CD69^+CD103^+$ (49.9% ± 23.9%) and $CD69^+CD103^-$ (25.1% ± 17.3%) $CD8^+$ T cells and low numbers of $CD69^-CD103^+$ (4.3% ± 5.3%) $CD8^+$ T cells (Figure 2C). In line with literature,[14,31] most tissue-resident $CD4^+$ T cells lack CD103 expression but express CD69 (55.3% ± 20.3%), which was also apparent in metastatic tumors (Figure 2D). Only 6.0% ± 5.2% and 1.7% ± 2.7% $CD4^+$ T cells were $CD69^+CD103^+$ or $CD69^-CD103^+$, respectively (Figure 2D). Intriguingly, the expression of tissue residency markers increased for both $CD8^+$ and $CD4^+$ T cells in late-stage tumors compared to that of early-stage tumors (Figure 2C and D). Thus, late-stage TILs decrease the Tem compartment and increase tissue residency traits.

Tissue-resident T cells from metastatic lesions express high levels of activation markers

To further define the fitness of the T cell infiltrates from late-stage NSCLC tumor lesions, we measured several exhaustion and activation markers. This included PD-1, a marker that correlates with the dysfunctional state of TILs.[32,33] In late-stage TILs, PD-1 levels reached 10.2% ± 14.4% for $CD8^+$ T cells (Figure 2E) and 8.8% ± 9.4% for conventional $CD4^+$ T cells (Figure 2F). These percentages did not significantly differ from those of early-stage tumors (Figure 2E and F).

Also the ectonucleoside triphosphate diphosphohydrolase-1 CD39 marks activated and exhausted T cells.[34-36] When combined with tissue residency markers CD69 and CD103, CD39 identifies T cells that can infiltrate human solid tumors.[36-39] Indeed, in metastatic tumors, CD39 was most prominently expressed in $CD103^+$ $CD8^+$ T cells, with an average expression of 41.5% ± 24.0% for $CD39^+CD103^+$ $CD8^+$ T cells compared to 11.1% ± 14.9% for $CD39^+CD103^-$ ($P < 0.0001$) and 8.5% ± 8.3% for $CD39^-CD103^+$ ($P < 0.0001$) (Figure 2G). In conventional $CD4^+$ T cells, CD39 expression was more evenly distributed between $CD39^+CD69^+$ (26.7% ± 16.3%), $CD39^+CD69^-$ (12.7% ± 7.0%) and $CD39^-CD69^+$ (30.4% ± 21.3%) $CD4^+$ T cells (Figure 2H).

We then turned to the costimulatory molecule CD137, which enriches for naturally occurring tumor-reactive T cells.[40] In metastatic NSCLC lesions, 13.9% ± 9.1% $CD8^+$ T cells and 6.1% ± 4.0% conventional $CD4^+$ T cells expressed CD137 (Figure 2I and J). Intriguingly, CD39−CD103 double expressing $CD8^+$ T cells enriched for CD137-expressing cells (28.7% ± 14.3%; Figure 2I; $P < 0.0001$). This was also true when CD69 was used as marker for tissue residency (Supplementary Figure S3A, available at https://doi.org/10.1016/j.iotech.2022.100090). For conventional $CD4^+$ T cells, similar trends of increased CD137 expression on $CD39^+$ T cells were detected (Figure 2J). Specifically, CD137 expression increased from 2.1% ± 1.9% on $CD69^+$ $CD4^+$ T cells to 9.9% ± 2.7% on $CD39^+CD69^+$ $CD4^+$ T cells, and to 8.8% ± 5.2% on $CD39^+$ single-positive cells (Figure 2J). Overall, late-stage NSCLC tumors contained higher percentages of Tcm cells at the expense of Tem cells. Tissue residency markers as well as the expression of CD39 and CD37 were increased on TILs, suggesting that tumor-responsive T cells are present in metastatic NSCLC lesions.

Effective TIL expansion from metastatic NSCLC tumors

Generating TIL products for the clinic requires effective TIL expansion. We therefore determined the expansion rate of TILs from metastatic lesions with the current gold standard, the clinically approved REP protocol.[22] During the first 10-13 days of culture with hrIL-2 (pre-REP), TILs expanded on average a 40-fold, which was slightly more than early-stage TILs (Figure 3A). During the REP of 10-13 days with anti-CD3 and IL-2, TILs expanded an additional 100-fold (Figure 3A), resulting in a total expansion rate of on average 3500-fold (Figure 3A). The total expansion rate was comparable to early-stage TILs (Figure 3A),[14] and was achieved for TILs originating from different metastatic locations (Figure 3B) and was overall independent from different pre-treatments (Figure 3C). Importantly, the amount of total viable cells per gram tissue we obtained after expansion was comparable with early-stage tumors (Figure 3D).[14] Also, using the tumor size (Table 2) to extrapolate tumor mass and to estimate the expansion rate from the total tumor lesion, all 27 TIL products would have resulted in $>1 \times 10^9$ cells (Figure 3D), a number that is compatible with TIL infusion into patients. Thus, effective TIL expansion can be achieved from late-stage metastatic NSCLC tumors independent of the metastatic location and/or previous treatments given to the patient.

We next measured the T cell content at the end of TIL expansion. Similar to early-stage NSCLC tumor lesions,[14] Foxp3-expressing T cells, were lost after expansion (Supplementary Figure S4, available at https://doi.org/10.1016/j.iotech.2022.100090). The percentage of $CD8^+$ T cells increased from 30% ± 16.3% in the tumor digest *ex vivo* to 58% ± 26.7% after REP ($P = 0.006$) (Figure 3E; for gating strategy, see Supplementary Figure S4, available at https://doi.org/10.1016/j.iotech.2022.100090). Conversely, the percentage of $CD4^+$ T cells remained constant (Figure 3E). The ratio of $CD8^+$ T cells over $CD4^+$ T cells increased from 1.3 *ex vivo* to 7.6 after REP (Figure 3F; $P = 0.04$). Expanded TILs thus primarily consist of $CD4^+$ and $CD8^+$ T cells.

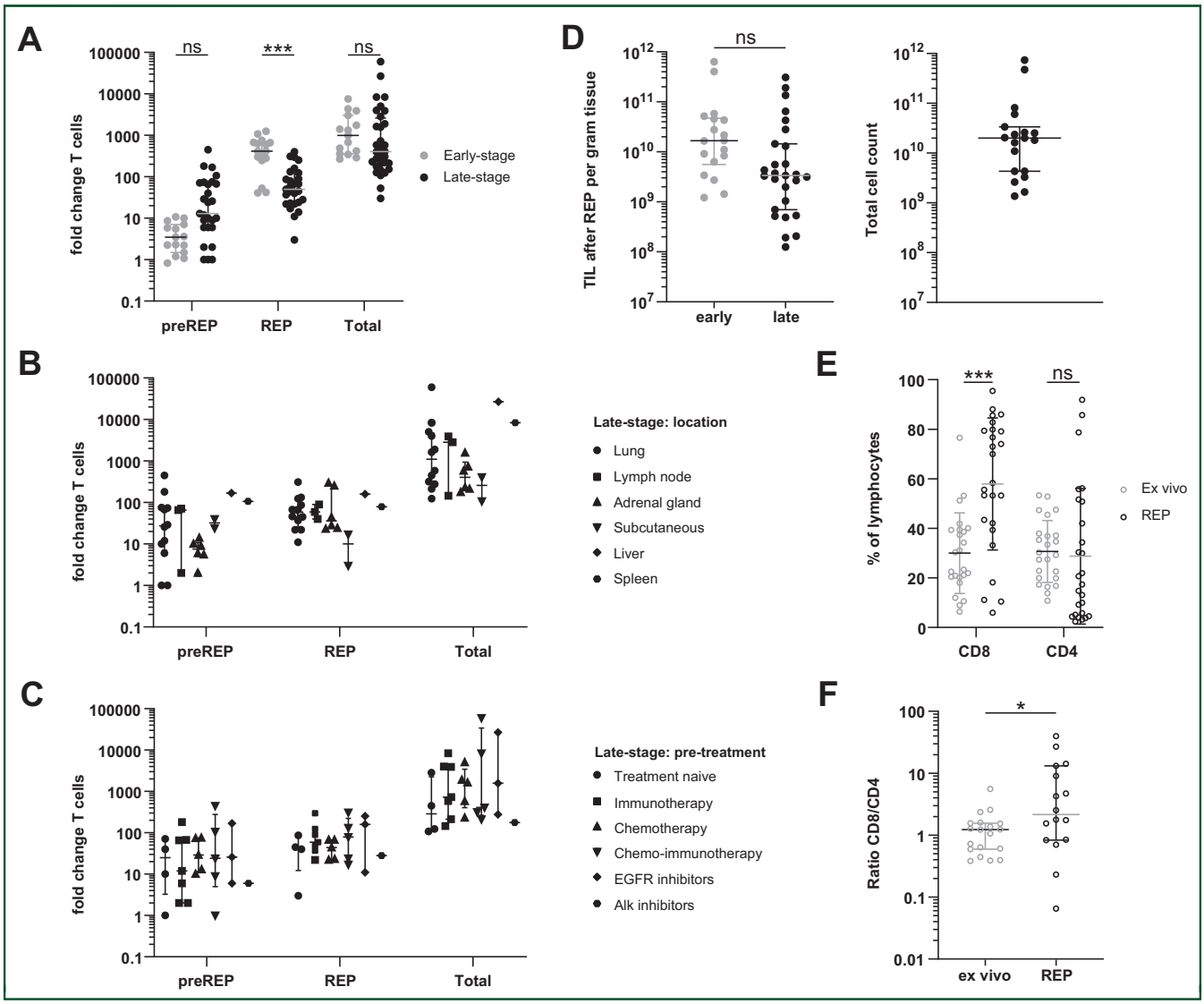

Figure 3. Efficient expansion of late-stage non-small-cell lung cancer (NSCLC) tumor-infiltrating T cells (TILs). Single-cell suspensions from tumor digests were cultured with 6000 IU interleukin 2 (IL-2) for 10-13 days [pre-rapid expansion phase (REP)], and then for an additional 10-13 days with irradiated feeder cells, 30 ng/ml OKT3 and 3000 IU IL-2 (REP). (A) Fold change of T cell numbers during pre-REP (left), REP (middle) and total expansion (right), compared between late-stage (black, $n = 27$) and early-stage (gray, $n = 15$)[14] NSCLC lesions. The number of life cells was determined with trypan blue staining. (B, C) Pre-REP (left), REP (middle) and total expansion (right) from (B) different tumor lesion sites and (C) different pre-treatment regimens. (D) Left: TIL count per gram tissue for the final TIL product after expansion, compared between late-stage (black, $n = 27$) and early-stage (gray, $n = 15$)[14] NSCLC lesions. Right: Total cell count after expansion for late-stage NSCLC lesions, based on the total tumor size and count per gram tissue after expansion. (E) $CD8^+$ T cell (left) and conventional $CD4^+$ T cell (right) as percentage of lymphocytes, compared between *ex vivo* (gray, $n = 27$) and REP (black, $n = 27$). (F) Ratio of $CD8^+$ T cells and conventional $CD4^+$ T cells, compared between *ex vivo* (gray, $n = 27$) and REP (black, $n = 27$). Each dot represents one patient. All graphs show median and 25th and 75th percentile interval. Significance was calculated with unpaired Student's *t*-test. $*P < 0.05$, $***P < 0.001$. Not significant (ns): $P \geq 0.05$. ALK, anaplastic lymphoma kinase; EGFR, epidermal growth factor receptor.

TIL products from metastatic lesions contain tumor-responsive cells

To study the functionality of TILs expanded from metastatic NSCLC lesions, we firstly measured their overall capacity to produce TNF, IFN-γ or IL-2 after 6 h of activation with PMA and ionomycin. Intriguingly, some TIL products produced high levels of one specific cytokine (Supplementary Figure S5, available at https://doi.org/10.1016/j.iotech.2022.100090), yet most produced two or more (Supplementary Figure S5, available at https://doi.org/10.1016/j.iotech.2022.100090), revealing their capacity to amply produce cytokines.

To define their tumor reactivity, we exposed TIL products for 6 h to the autologous tumor digest if available ($n = 21$), or with medium alone as control, and we measured the TNF, IFN-γ, IL-2 production and CD137 expression (Figure 4A, Supplementary Figure S6, available at https://doi.org/10.1016/j.iotech.2022.100090). To distinguish the expanded TILs from T cell infiltrates of the tumor digest, we pre-stained the expanded TILs with CD4 and CD8 antibodies before the co-culture. TIL products contained $CD8^+$ and $CD4^+$ T cells that produced TNF, IFN-γ, IL-2 or that expressed CD137 in response to tumor digest (Figure 4B). The sum of $CD8^+$ T cells producing at least one cytokine or

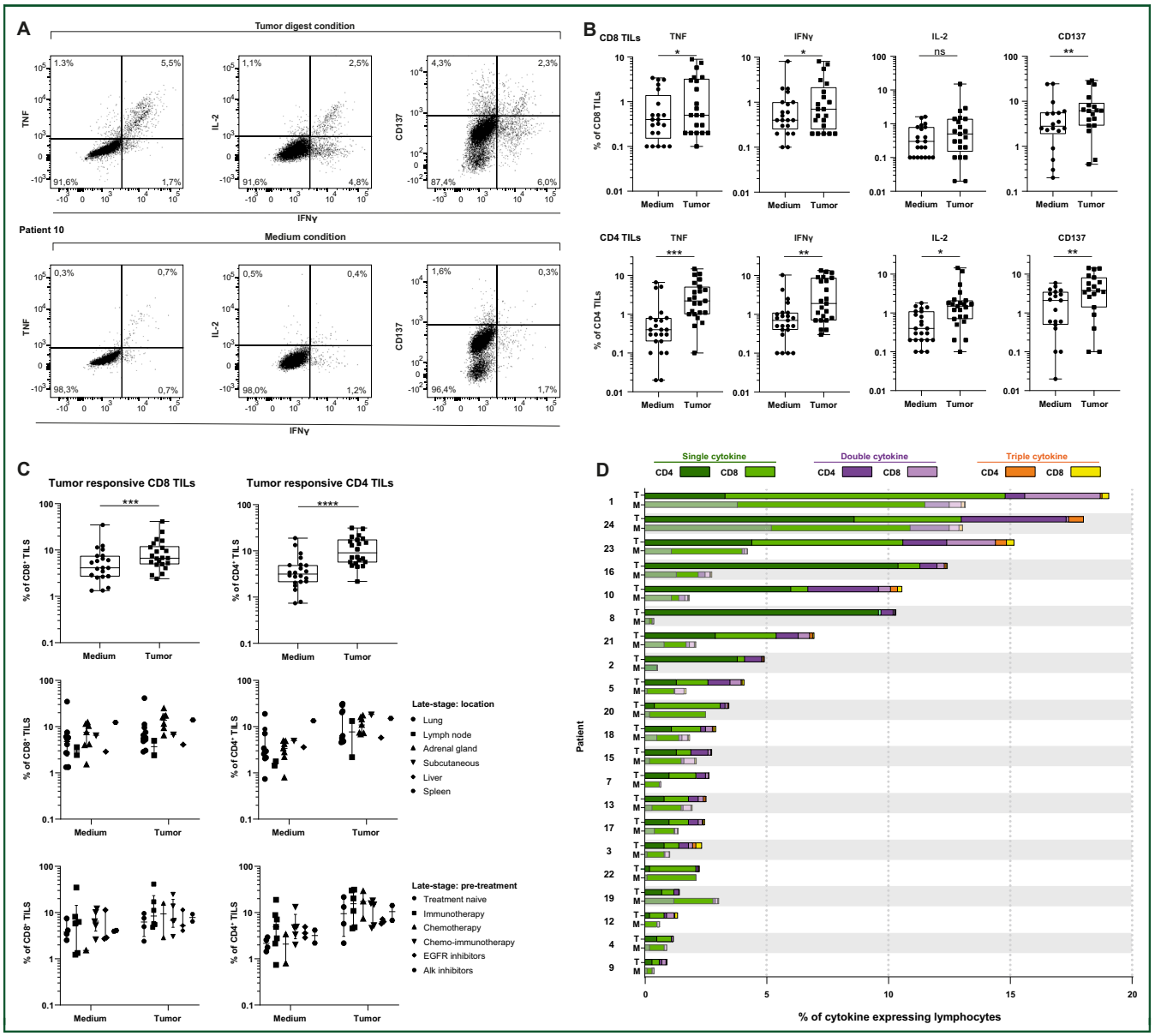

Figure 4. Expanded tumor-infiltrating T cells (TILs) produce pro-inflammatory cytokines and express CD137 in response to autologous tumor digest. TIL products generated from 22 patients were stained with fluorescently labeled $CD4^+$ and $CD8^+$ antibodies before co-culture with autologous tumor digest or medium for 6 h at 37°C. Cytokine production and CD137 expression were defined by flow cytometry. (A) Gating strategy for the TILs exposed to tumor digest (top) or to medium (bottom) (patient 10), based on the expression of interferon (IFN)-γ (x-axis) and tumor necrosis factor (TNF), interleukin 2 (IL-2) and CD137 (y-axis). (B) Representative plots showing percentage of positive $CD8^+$ (top) and $CD4^+$ (bottom) TILs for TNF, IFN-γ, IL-2 and CD137 of tumor-exposed TILs (left) compared to medium control (right). (C) Percentage of tumor-responsive $CD8^+$ (left) and $CD4^+$ (right) TILs. Tumor responsiveness was defined on the expression of at least one of the markers, i.e. TNF, IFN-γ, IL-2 and CD137 (top), and also compared between different tumor lesion sites (middle) and different pre-treatment regimens (bottom). (D) Percentage of cytokine-producing TILs that produce one, two or three cytokines simultaneously upon exposure to tumor digest (top bar) or to medium (lower bar). A-C: Each dot represents one patient. D: Each bar represents one patient, patient number corresponds to Table 1. Graphs in B and C show median and 25th and 75th percentile interval. Significance was calculated with paired Student's *t*-test. $*P < 0.05$, $**P < 0.01$, $***P < 0.001$, $****P < 0.0001$. Not significant (ns): $P \geq 0.05$.

CD137 (labeled as tumor-responsive) reached 10.0% ± 8.9% in response to tumor digest, compared to 6.6% ± 7.2% positive cells in the medium control (Figure 4C; $P = 0.0007$). With 13.0% ± 8.8% of tumor-responsive cells compared to 4.5% ± 4.3% in medium control, $CD4^+$ TILs were more tumor-responsive (Figure 4C; $P < 0.0001$). The level of tumor-responsive TILs could not be attributed to metastatic location or pre-treatment (Figure 4C).

We next divided tumor-reactive $CD8^+$ and $CD4^+$ T cells into single cytokine producers, double producers (i.e. that produce two of the three measured cytokines) and triple producers (i.e. that produce all three measured cytokines) (Figure 4D). Even though single cytokine producers contributed most, almost all TIL products contained double and triple cytokine-producing TILs above background (medium control) (Figure 4D). Notably, polyfunctional T cells were present in 16 out of 21 (76%) TIL products, including those with a low percentage of cytokine-producing T cells (Figure 4D). Thus, albeit at different levels, most TIL products contain cytokine-producing, CD137-expressing T cells.

DISCUSSION

Here, we showed that tumor-reactive TILs can be efficiently isolated and expanded from metastatic NSCLC tumors, irrespective of their location and the pre-treatment regimen. An important parameter to generate TIL products is the presence of T cells. Previous studies proposed that the tissue origin from tumor shapes the metastatic immune cell composition.[41] Indeed, the frequency of $CD8^+$ TILs in metastatic renal cell carcinomas and colorectal tumors was comparable to their primary tumors.[42] With the exception of brain metastasis,[43,44] which was not included in our cohort, the overall lymphocyte infiltration in metastatic NSCLC lesions also closely resembled that of primary tumors.[14] Specifically, the distribution of $CD8^+$ T cells, conventional $CD4^+$ T cells and Tregs was similar, just like the percentages of B cells, NK cells and NKT cells. Our cohort mainly consisted of adenocarcinoma tumors (Table 2), prohibiting us from comparing different tumor subtypes. Nonetheless, our data indicate that all metastatic lesion sites tested allowed for generating TIL products for therapeutic purposes.

In line with their well-established antitumoral cytolytic function,[45-48] most TIL products generated from metastatic lesions contained antitumoral $CD8^+$ T cell responses, as defined by cytokine production and/or CD137 expression after co-culture with autologous tumor digest. Intriguingly, $CD4^+$ T cells responded more robustly to autologous tumor digest, a feature not observed in early-stage NSCLC tumors.[14] Several recent studies identified antitumoral cytolytic $CD4^+$ T cell responses in solid tumors, including NSCLC.[49-53] Therefore, we hypothesize that $CD4^+$ T cell responses could also substantially contribute to the antitumoral responses against NSCLCs. Importantly, 76% ($n = 16$) of TIL products contained polyfunctional T cells, considered the most potent antitumoral T cells.[25,26,54] Thus, the generated TIL products should achieve antitumoral responses.

Another important point is if tumor lesions with a high likelihood of containing tumor-specific T cells can be identified before expansion. We and others showed a correlation between high PD-1 expression on TILs and antitumor responses in TIL products.[14,55] Unfortunately, circulating anti-PD-1/programmed death ligand-1 antibodies in nivolumab and/or pembrolizumab-treated patients (anti-PD-1 immunotherapy) impede such expression analysis for many patients in our cohort. However, other markers may help identify tumor-responsive TILs in such a patient cohort. The number of tissue-resident $CD103^+$ and CD69 $CD8^+$ T cells and of $CD69^+$ $CD4^+$ T cells was increased in late-stage tumors. Furthermore, these tissue-resident TILs showed increased expression of CD39 and CD137, which is indicative for TCR engagement and thus potentially for tumor-specific TILs.[38,40,56] $CD137^+$ TILs express the highest levels of IFN-γ, TNF and IL-2,[40,57,58] which may further point to their tumor reactivity. It is therefore tempting to speculate that CD103, CD69, CD39 and CD137 combined could identify and potentially even enrich for tumor-specific TILs.

TIL therapy demonstrated its potential in late-stage melanoma,[20,22,59] bladder cancer,[60] breast cancer,[61] ovarian cancer,[62] head and neck cancer[63] and recently also for NSCLC.[27] In anti-PD-1-refractory NSCLC patients, 11 out of 16 patients (76%) showed an objective response, and 2 a complete response, which highlights the potential of TIL therapy for NSCLC patients.[27] Importantly, as for melanoma alike,[64] this study revealed that TIL therapy is beneficial in patients who failed immunotherapy. Our cohort is too small to extract differences in TIL expansion and tumor reactivity in patient subgroups based on different pre-treatment regimens or metastatic lesion sites. Nonetheless, none of the specific pre-treatment regimen or the tested locations of metastatic lesions should exclude a patient from receiving TIL therapy. However, because TIL therapy is less effective when used as second- or third-line treatment,[65] it is key to identify the most suitable therapy early on, and to consider TIL therapy as first-line treatment.

In conclusion, we showed that the generation of tumor-reactive TIL products from late-stage NSCLC tumors is feasible, irrespective of pre-treatment regimen or tumor origin. TIL products reach sufficient cell numbers for clinical application, and most display polyfunctional antitumor effector functions. We are therefore confident that TIL therapy will generate promising results for metastatic NSCLC patients in upcoming clinical trials.

ACKNOWLEDGEMENTS

We thank the flow cytometry facility from Sanquin Research, and the medical assistance staff from the NKI-AvL for technical help.

FUNDING

This research was supported by intramural funding of Sanquin: Stichting Sanquin Bloedvoorziening [grant number PPOC 19-04].

DISCLOSURE

Given their role as a Editor-in-Chief, John Haanen had no involvement in the peer review of this article and has no access to information regarding its peer review. Full responsibility for the editorial process for this article was delegated to Samra Turajlic, Associate Editor, of the Journal. The authors have declared no conflicts of interest.

REFERENCES

1. WHO. Cancer. 2020. Available at https://www.who.int/news-room/fact-sheets/detail/cancer. Accessed August 26, 2021.
2. Siegel R, Miller K, Jemal A. Cancer statistics, 2020. *CA Cancer J Clin*. 2020;70(1):7-30.
3. Yoneda K, Imanishi N, Ichiki Y, Tanaka F. Treatment of non-small cell lung cancer with EGFR-mutations. *J UOEH*. 2019;41(2):153-163.
4. Recondo G, Facchinetti F, Olaussen KA, Besse B, Friboulet L. Making the first move in EGFR-driven or ALK-driven NSCLC: first-generation or next-generation TKI? *Nat Rev Clin Oncol*. 2018;15(11):694-708.
5. Smit EF, de Langen AJ. Pembrolizumab for all PD-L1-positive NSCLC. *Lancet*. 2019;393(10183):1776-1778.

6. Sui H, Ma N, Wang Y, et al. Anti-PD-1/PD-L1 therapy for non-small-cell lung cancer: toward personalized medicine and combination strategies. *J Immunol Res*. 2018;2018:6984948.
7. Reck M, Rodríguez-Abreu D, Robinson AG, et al. Pembrolizumab versus chemotherapy for PD-L1-positive non-small-cell lung cancer. *N Engl J Med*. 2016;375(19):1823-1833.
8. Yuan M, Huang LL, Chen JH, Wu J, Xu Q. The emerging treatment landscape of targeted therapy in non-small-cell lung cancer. *Signal Transduct Target Ther*. 2019;4(1):61.
9. Mulherkar R, Grewal AS, Berman AT. Emerging role of immunotherapy in locally advanced non-small cell lung cancer. *Clin Adv Hematol Oncol*. 2020;18:212-217.
10. Ko E, Raben D, Formenti S. The integration of radiotherapy with immunotherapy for the treatment of non-small cell lung cancer. *Clin Cancer Res*. 2018;24(23):5792-5806.
11. Mielgo-Rubio X, Uribelarrea EA, Cortés LQ, Moyano MS. Immunotherapy in non-small cell lung cancer: update and new insights. *J Clin Transl Res*. 2021;7(1):1.
12. Lung ASCO. Cancer-Non-Small Cell: Statistics. Cancer.Net. Available at https://www.cancer.net/cancer-types/lung-cancer-non-small-cell/statistics. Accessed August 26, 2021.
13. Alexandrov LB, Nik-Zainal S, Wedge DC, et al. Signatures of mutational processes in human cancer. *Nature*. 2013;500(7463):415-421.
14. De Groot R, Van Loenen MM, Guislain A, et al. Polyfunctional tumor-reactive T cells are effectively expanded from non-small cell lung cancers, and correlate with an immune-engaged T cell profile. *Oncoimmunology*. 2019;8(11):e1648170.
15. Kargl J, Busch SE, Yang GHY, et al. Neutrophils dominate the immune cell composition in non-small cell lung cancer. *Nat Commun*. 2017;8:14381.
16. Kataki A, Scheid P, Piet M, et al. Tumor infiltrating lymphocytes and macrophages have a potential dual role in lung cancer by supporting both host-defense and tumor progression. *J Lab Clin Med*. 2002;140(5):320-328.
17. Farhood B, Najafi M, Mortezaee K. CD8 + cytotoxic T lymphocytes in cancer immunotherapy: a review. *J Cell Physiol*. 2019;234(6):8509-8521.
18. Oh DY, Kwek SS, Raju SS, et al. Intratumoral CD4 + T cells mediate anti-tumor cytotoxicity in human bladder cancer. *Cell*. 2020;181(7):1612-1625.e13.
19. Rosenberg SA, Restifo NP. Adoptive cell transfer as personalized immunotherapy for human cancer. *Science*. 2015;348(6230):62-68.
20. Rosenberg SA, Dudley ME. Adoptive cell therapy for the treatment of patients with metastatic melanoma. *Curr Opin Immunol*. 2009;21(2):233.
21. Hong JJ, Rosenberg SA, Dudley ME, et al. Successful treatment of melanoma brain metastases with adoptive cell therapy. *Clin Cancer Res*. 2010;16(19):4892-4898.
22. van den Berg JH, Heemskerk B, van Rooij N, et al. Tumor infiltrating lymphocytes (TIL) therapy in metastatic melanoma: boosting of neoantigen-specific T cell reactivity and long-term follow-up. *J Immunother Cancer*. 2020;8(2):e000848.
23. Sarnaik AA, Hamid O, Khushalani NI, et al. Lifileucel, a tumor-infiltrating lymphocyte therapy, in metastatic melanoma. *J Clin Oncol*. 2021;39(24):2656-2666.
24. van Asten SD, de Groot R, van Loenen MM, et al. T cells expanded from renal cell carcinoma display tumor-specific CD137 expression but lack significant IFN-γ, TNF-α or IL-2 production. *Oncoimmunology*. 2021;10(1):1860482.
25. Donia M, Kjeldsen JW, Andersen R, et al. PD-1 + polyfunctional T cells dominate the periphery after tumor-infiltrating lymphocyte therapy for cancer. *Clin Cancer Res*. 2017;23(19):5779-5788.
26. Wimmers F, Aarntzen EHJG, Duiveman-deBoer T, et al. Long-lasting multifunctional CD8 + T cell responses in end-stage melanoma patients can be induced by dendritic cell vaccination. *Oncoimmunology*. 2015;5(1).
27. Creelan BC, Wang C, Teer JK, et al. Tumor-infiltrating lymphocyte treatment for anti-PD-1-resistant metastatic lung cancer: a phase 1 trial. *Nat Med*. 2021;27(8):1410-1418.
28. Melioli G, Ratto G, Guastella M, et al. Isolation and in vitro expansion of lymphocytes infiltrating non-small cell lung carcinoma: functional and molecular characterisation for their use in adoptive immunotherapy. *Eur J Cancer*. 1994;30(1):97-102.
29. Tamura T, Kurishima K, Nakazawa K, et al. Specific organ metastases and survival in metastatic non-small-cell lung cancer. *Mol Clin Oncol*. 2015;3(1):217.
30. Amsen D, van Gisbergen KPJM, Hombrink P, van Lier RAW. Tissue-resident memory T cells at the center of immunity to solid tumors. *Nat Immunol*. 2018;19(6):538-546.
31. Oja AE, Piet B, van der Zwan D, et al. Functional heterogeneity of CD4 + tumor-infiltrating lymphocytes with a resident memory phenotype in NSCLC. *Front Immunol*. 2018;9:2654.
32. Thommen DS, Schumacher TN. T cell dysfunction in cancer. *Cancer Cell*. 2018;33(4):547.
33. Ahmadzadeh M, Johnson LA, Heemskerk B, et al. Tumor antigen-specific CD8 T cells infiltrating the tumor express high levels of PD-1 and are functionally impaired. *Blood*. 2009;114(8):1537.
34. Allard D, Allard B, Stagg J. On the mechanism of anti-CD39 immune checkpoint therapy. *J Immunother Cancer*. 2020;8(1):e000186.
35. Kortekaas KE, Santegoets SJ, Sturm G, et al. CD39 identifies the CD4 + tumor-specific T-cell population in human cancer. *Cancer Immunol Res*. 2020;8(10):1311-1321.
36. O'Brien SM, Klampatsa A, Thompson JC, et al. Function of human tumor-infiltrating lymphocytes in early stage non-small cell lung cancer. *Cancer Immunol Res*. 2019;7(6):896-909.
37. Timperi E, Barnaba V. CD39 regulation and functions in T cells. *Int J Mol Sci*. 2021;22(15):8068.
38. Duhen T, Duhen R, Montler R, et al. Co-expression of CD39 and CD103 identifies tumor-reactive CD8 T cells in human solid tumors. *Nat Commun*. 2018;9(1).
39. Scheper W, Kelderman S, Fanchi LF, et al. Low and variable tumor reactivity of the intratumoral TCR repertoire in human cancers. *Nat Med*. 2018;25(1):89-94.
40. Ye Q, Song DG, Poussin M, et al. CD137 accurately identifies and enriches for naturally occurring tumor-reactive T cells in tumor. *Clin Cancer Res*. 2014;20(1):44-55.
41. DeNardo DG, Johansson M, Coussens LM. Immune cells as mediators of solid tumor metastasis. *Cancer Metastasis Rev*. 2008;27(1):11-18.
42. Remark R, Alifano M, Cremer I, et al. Characteristics and clinical impacts of the immune environments in colorectal and renal cell carcinoma lung metastases: influence of tumor origin. *Clin Cancer Res*. 2013;19(15):4079-4091.
43. García-Mulero S, Alonso MH, Pardo J, et al. Lung metastases share common immune features regardless of primary tumor origin. *J Immunother Cancer*. 2020;8(1):e000491.
44. Ikarashi D, Okimoto T, Shukuya T, et al. Comparison of tumor microenvironments between primary tumors and brain metastases in patients with NSCLC. *JTO Clin Res Rep*. 2021;2(10):100230.
45. Nicolet BP, Guislain A, van Alphen FPJ, et al. CD29 identifies IFN-γ-producing human CD8 + T cells with an increased cytotoxic potential. *Proc Natl Acad Sci U S A*. 2020;117(12):6686-6696.
46. Corgnac S, Boutet M, Kfoury M, Naltet C, Mami-Chouaib F. The emerging role of CD8 + tissue resident memory T (T RM) cells in antitumor immunity: a unique functional contribution of the CD103 integrin. *Front Immunol*. 2018;9:1904.
47. Sawada M, Goto K, Morimoto-Okazawa A, et al. PD-1+ Tim3+ tumor-infiltrating CD8 T cells sustain the potential for IFN-γ production, but lose cytotoxic activity in ovarian cancer. *Int Immunol*. 2020;32(6):397-405.
48. Gallerano D, Ciminati S, Grimaldi A, et al. Genetically driven CD39 expression shapes human tumor-infiltrating CD8 + T-cell functions. *Int J Cancer*. 2020;147(9):2597-2610.
49. Nicolet BP, Guislain A, Wolkers MC. CD29 enriches for cytotoxic human CD4+ T cells. *J Immunol*. 2021;207(12):2966-2975.
50. Oja AE, Braga FAV, Remmerswaal EBM, et al. The transcription factor Hobit identifies human cytotoxic CD4 + T cells. *Front Immunol*. 2017;8:325.
51. Linnemann C, van Buuren MM, Bies L, et al. High-throughput epitope discovery reveals frequent recognition of neo-antigens by CD4+ T cells in human melanoma. *Nat Med*. 2014;21(1):81-85.

52. Cachot A, Bilous M, Liu YC, et al. Tumor-specific cytolytic CD4 T cells mediate immunity against human cancer. *Sci Adv*. 2021;7(9).
53. Veatch JR, Jesernig BL, Kargl J, et al. Endogenous CD4+ T cells recognize neoantigens in lung cancer patients, including recurrent oncogenic KRAS and ERBB2 (Her2) driver mutations. *Cancer Immunol Res*. 2019;7(6):910-922.
54. Seder RA, Darrah PA, Roederer M. T-cell quality in memory and protection: implications for vaccine design. *Nat Rev Immunol*. 2008;8(4):247-258.
55. Thommen DS, Koelzer VH, Herzig P, et al. A transcriptionally and functionally distinct PD-1+ CD8+ T cell pool with predictive potential in non-small-cell lung cancer treated with PD-1 blockade. *Nat Med*. 2018;24(7):994-1004.
56. Datar I, Sanmamed MF, Wang J, et al. Expression analysis and significance of PD-1, LAG-3, and TIM-3 in human non-small cell lung cancer using spatially resolved and multiparametric single-cell analysis. *Clin Cancer Res*. 2019;25(15):4663-4673.
57. Hodge G, Holmes M, Jersmann H, Reynolds PN, Hodge S. Targeting peripheral blood pro-inflammatory cytotoxic lymphocytes by inhibiting CD137 expression: novel potential treatment for COPD. *BMC Pulm Med*. 2014;14(1):85.
58. Akhmetzyanova I, Zelinskyy G, Littwitz-Salomon E, et al. CD137 agonist therapy can reprogram regulatory T cells into cytotoxic CD4+ T cells with antitumor activity. *J Immunol*. 2016;196(1):484-492.
59. Besser MJ, Shapira-Frommer R, Itzhaki O, et al. Adoptive transfer of tumor-infiltrating lymphocytes in patients with metastatic melanoma: intent-to-treat analysis and efficacy after failure to prior immunotherapies. *Clin Cancer Res*. 2013;19(17):4792-4800.
60. Poch M, Hall M, Joerger A, et al. Expansion of tumor infiltrating lymphocytes (TIL) from bladder cancer. *Oncoimmunology*. 2018;7(9):e1476816.
61. Autologous Tumor Infiltrating Lymphocytes in Patients With Pretreated Metastatic Triple Negative Breast Cancer—Full Text View—ClinicalTrials.gov. Available at https://clinicaltrials.gov/ct2/show/study/NCT04111510. Accessed December 21, 2021.
62. Pedersen M, Westergaard MCW, Milne K, et al. Adoptive cell therapy with tumor-infiltrating lymphocytes in patients with metastatic ovarian cancer: a pilot study. *Oncoimmunology*. 2018;7(12):e1502905.
63. Adoptive Cell Transfer of Autologous Tumor Infiltrating Lymphocytes and High-Dose Interleukin 2 in Select Solid Tumors—Full Text View—ClinicalTrials.gov. Available at https://clinicaltrials.gov/ct2/show/NCT03991741. Accessed December 21, 2021.
64. Andersen R, Borch TH, Draghi A, et al. T cells isolated from patients with checkpoint inhibitor-resistant melanoma are functional and can mediate tumor regression. *Ann Oncol*. 2018;29(7):1575-1581.
65. Seitter SJ, Sherry RM, Yang JC, et al. Impact of prior treatment on the efficacy of adoptive transfer of tumor-infiltrating lymphocytes in patients with metastatic melanoma. *Clin Cancer Res*. 2021;27:5289.